Gold Bull (2016) 49:103–109
DOI 10.1007/s13404-016-0185-5

ORIGINAL PAPER

Facile synthesis of Ag@Fe_3O_4@C-Au core-shell microspheres for surface-enhanced Raman scattering

Mao Shen[1] · Suqing Chen[1] · Wenping Jia[1] · Guodong Fan[2] · Yanxian Jin[1] · Huading Liang[1]

Received: 18 October 2015 / Accepted: 24 October 2016 / Published online: 15 November 2016

Abstract In this paper, a facile approach has been developed to synthesize the novel multifunctional Ag@Fe_3O_4@C-Au magnetic core-shell microspheres that display a highly efficient surface-enhanced Raman scattering (SERS) substrate with high stability and reproducibility. The morphology, size, chemical component, and magnetic property of as-prepared composite microspheres were characterized by scanning transmission electron microscopy (SEM), transmission electron microscopy (TEM), X-ray diffraction (XRD), thermogravimetric analysis (TGA), X-ray photoelectron spectra (XPS), and vibrating sample magnetomerter (VSM), respectively. The enhancement effect on the Raman active was investigated by using rhodamine-b (RdB) as a probe molecule. The result shows that the well-designed Ag@Fe_3O_4@C-Au core-shell microspheres have uniform sphere size and high magnetization, and the SERS signals of RdB on the Ag@Fe_3O_4@C-Au microspheres were much stronger than those on both Ag@Fe_3O_4 and Fe_3O_4@C-Au microspheres.

Keywords Magnetic nanoparticles · Noble metal · SERS · Core-shell

Introduction

Surface-enhanced Raman scattering spectroscopy (SERS) is a highly sensitive and selective tool that provides fine details of molecules through high-quality spectra, primarily due to the large electromagnetic enhancement (EM) of the localized surface plasmon resonance (LSPR) in nanostructures. Since its first observation in the 1970s [1], SERS has been employed increasing toward microanalytical applications in various fields due to it being 10^6–10^8 times more sensitive than conventional Raman. Generally, substrates based on metals such as Au, Ag, and their composites are required to realize a substantial SERS effect [2–5]. But, it is widely known that surface plasmon efficiency is greater for Ag than it is for Au [6]. In addition, Ag is more mobile and more easily oxidized than Au. If Ag nanostructures can be stabilized by a chemically and electrically inert shell, these weaknesses can be managed. So, Kim et al. developed an Ag-silica-Au hybrid device that displayed a long-range plasmon transfer of Ag to Au leading to enhanced Raman scattering of molecules largely separated from the optically excited Ag surface [7]. On the other hand, despite there are many advantages of long-range plasmon transfer of Ag to Au leading to enhanced Raman scattering, it must be emphasized that most of these SERS substrates are thrown away after detecting probably. Thus, it is of considerable importance to develop an efficient SERS substrate that can not only provide strong enhancement factors but also show high stability and reproducibility. To resolve this problem, magnetic materials such as Fe_3O_4 were introduced usually with Au or Ag nanoparticles to form composite structures for SERS substrates. In the past few years, various research groups have shown that such magnetic-core noble metal-shell composites not only are biocompatible but also facilitate large-scale Raman scattering enhancements [8–11]. For instance, Shen et al. report a novel multifunctional Fe_3O_4@ Ag/SiO_2/Au core-shell nanoparticles that display

---

✉ Huading Liang
lianghuading@tzc.edu.cn

[1] College of Pharmaceutical and Chemical Engineering, Taizhou University, Taizhou, Zhejiang 318000, People's Republic of China

[2] Key Laboratory of Auxiliary Chemistry and Technology for Chemical Industry, Ministry of Education, Shanxi University of Science and Technology, Xi'an 710021, People's Republic of China

long-range plasmon transfer of Ag to Au leading to enhanced Raman scattering [6]. Wang et al. synthesized Fe_3O_4/Ag/Au composites for immunoassay based on surface plasmon resonance biosensor [12].

In this work, we report the fabrication of a new kind of multifunctional Ag@Fe_3O_4@C-Au magnetic core-shell microspheres. The detailed protocol for the preparation of the Ag@Fe_3O_4@C-Au magnetic core-shell microspheres and detection of the rhodamine-b (RdB) is shown in Scheme 1. The well-designed microspheres have high magnetization and uniform sphere size. The SERS activities of these microspheres have been tested by using RdB as a probe molecule. The unique nanostructure makes the microspheres novel stable, reproducible, and a high-enhancement effect for Raman detection.

Experimental

Materials

Ethylene glycol (EG), anhydrous sodium acetate (NaOAc), iron nitrate ($Fe(NO_3)_3 \cdot 9H_2O$), silver nitrate ($AgNO_3$), poly(-vinyl-pyrrolidone) (PVP MW = 30,000), and polyetherimide (PEI) were obtained from the Tianjin Guangfu Fine Chemical Research Institute. Chloroauric acid ($HAuCl_4 \cdot 4H_2O$), ethanol, and RdB were purchased from Sinopharm Chemical Reagent Co.; 1-[3-(dimethylamino)propyl]-3-ethylcarbodii-mide hydrochloride (EDC), and N-hydroxy-succinimide (NHS) were purchased from Sigma Aldrich Co. All reagents were used as received without further purication. The pure water was obtained from a Milli-Q synthesis system.

Synthesis of Ag@Fe_3O_4 nanospheres

Functionalized Ag@Fe_3O_4 nanoparticles were synthesized via a versatile solvothermal reaction reported with a slight modification [13]. Briefly, $Fe(NO_3)_3 \cdot 9H_2O$ (1.5 g), NaOAc (3.5 g), PVP (1.0 g), and $AgNO_3$ (0.15 g) were dissolved in EG (70 ml) with magnetic stirring, followed by the transfer of the resulting mixture into a 100-ml Teflon-lined stainless-steel autoclave and heated at 200°C for 8 h. Finally, the products were collected with a magnet and dried in a vacuum oven at 60°C for further use.

Synthesis of Ag@Fe_3O_4@C nanospheres

The carboxyl and negative charge-functionalized magnetic Ag@Fe_3O_4@C nanospheres were obtained following the method reported [14]; 0.1 g Ag@Fe_3O_4 nanoparticles and 1.0 g glucose were immersed in 70 ml deionized water by ultrasonication for 30 min. Then, the solution was transferred to a 100-ml Teflon-sealed autoclave for treated at 200°C for 12 h. The products were separated by a magnet, and washed several times with ethanol and deionized water. Last, the as-obtained products were dried at 60°C for further use.

Loading Au nanoparticles to obtain Ag@ Fe_3O_4@C-Au nanospheres

Citrate-stabilized Au nanoparticles of about 16 nm were prepared according to the reported methods [15]. The deposition of Au nanoparticles onto Ag@Fe_3O_4@C was performed as follows. First, 0.1 g of Ag@Fe_3O_4@C was dispersed into 100-ml (0.5 mg/ml) PEI aqueous solution under magnetic stirring for 2 h; then, EDC (0.83 mmol) and NHS (0.83 mmol) were added into the solution under magnetic stirring for 12 h. The residual PEI was removed by magnetic separation, and the composites were rinsed with water at least three times. Last, Ag@Fe_3O_4@C-PEI microspheres was dispersed into 100-ml Au NP solution (0.48 mmol/l), and the dispersion was stirred for 4 h. Then, the precipitate

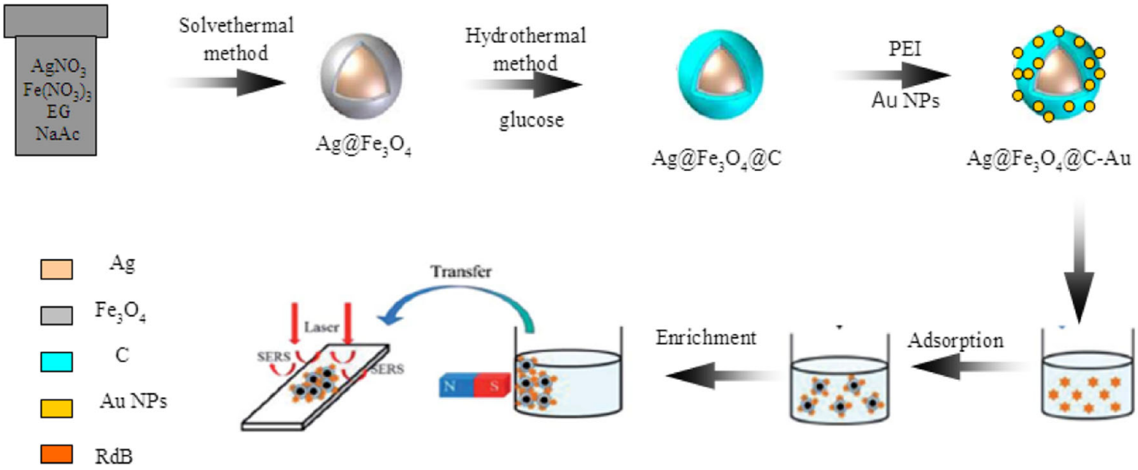

Scheme 1 The preparation procedure of the Ag@Fe_3O_4@C-Au microspheres and detection of the RdB

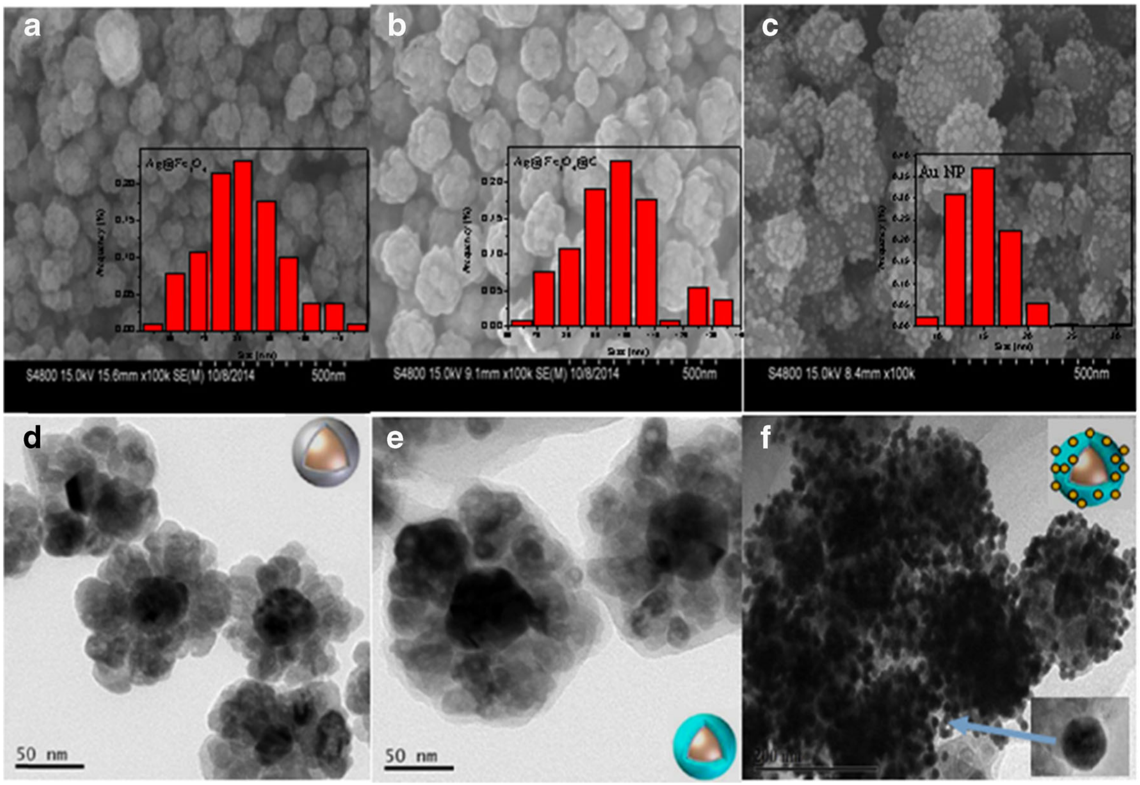

Fig. 1 SEM and TEM images of $Ag@Fe_3O_4$ (**a**, **d**), $Ag@Fe_3O_4@C$ (**b**, **e**), and $Ag@Fe_3O_4@C\text{-}Au$ (**c**, **f**) nanocomposites, respectively.

was collected by magnetic separation, washed several times with deionized water.

Measurements of SERS activity of the $Ag@Fe_3O_4@C\text{-}Au$ microspheres

RdB was used as a model molecule and Raman label for examination of the SERS activity of the $Ag@Fe_3O_4@C\text{-}Au$, $Ag@Fe_3O_4$, and $Fe_3O_4@C\text{-}Au$ microspheres, respectively. In a typical experiment, 10 mg of the as-prepared microspheres were dispersed in 10-ml ethanol solution of 10^{-8} M concentrations of RdB aqueous solution for 12 h under ambient temperature with vigorous shaking. Then, in situ SERS activity of the solution at the position of the magnet was detected, and a 633-nm laser was used for the Raman measurements.

Characterization

Transmission electron microscopy (TEM) images were obtained on a JEM-2100 TEM (Jeol Ltd., Tokyo, Japan). X-ray powder diffraction (XRD) analysis was performed using a Dmax-2500 (CuKα = 1.5406 Å; Rigaku Corporation, Tokyo, Japan). Magnetic characteristics were studied using a vibrating sample magnetometer (VSM) (Lake Shore Company, Westerville, OH, USA) at room temperature. Scanning transmission electron microscopy (SEM) was carried out on an S-4800 microscope (Hitachi Limited, Tokyo, Japan). Thermogravimetric analysis (TGA) of nanocomposite was performed on the TGA Q500 from TA Instruments (New Castle, DE, USA). Analyzed samples were heated from 100 to 800°C at a heating rate of 10°C/min. X-ray photoelectron spectra (XPS) were recorded by Thermo ESCALAB 250XI X-ray photoelectron spectrometer (Thermo Fisher Scientific Inc., Waltham, MA, USA) with nonmonochromatized Al Kα radiation as excitation source. Raman spectra were recorded

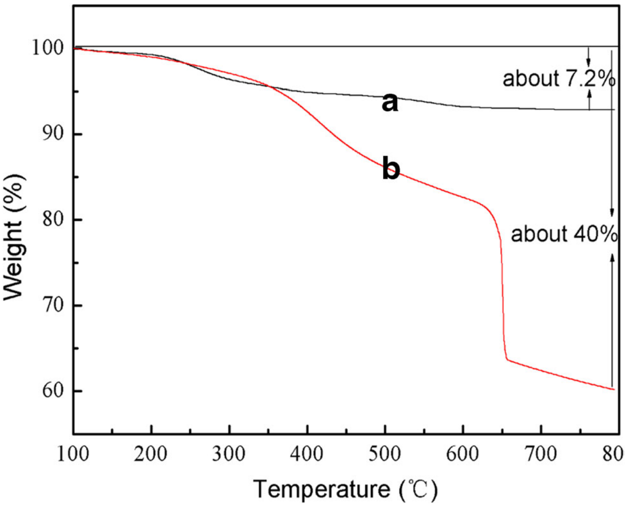

Fig. 2 TGA curves of naked Fe_3O_4 nanospheres (**a**) and $Ag@Fe_3O_4@C$ nanospheres (**b**)

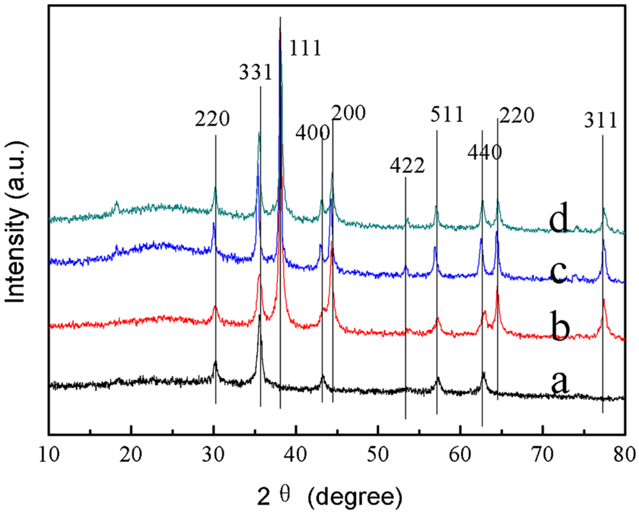

Fig. 3 Wide-angle XRD patterns of naked Fe_3O_4 nanospheres (**a**), $Ag@Fe_3O_4$ nanospheres (**b**), $Ag@Fe_3O_4@C$ nanospheres (**c**), and $Ag@Fe_3O_4@C$-Au nanospheres (**d**)

on a HR800 Raman microprobe (Horiba Jobin Yvon LabRAM, France) with 633-nm laser excitation.

Results and discussion

The shape and size of the as-prepared microspheres were examined by SEM and TEM. Figure 1a shows SEM image, which clearly indicates that the as-prepared $Ag@Fe_3O_4$ nanocomposite has a typical spherical nanostructure. All the particles are uniform and well dispersed without any large aggregations. The average diameter of the nanospheres is around 90 nm, and the surface of the particles is rough. The morphology of the $Ag@Fe_3O_4$ nanospheres is also clearly demonstrated from the TEM image. As shown in Fig. 1d, the $Ag@Fe_3O_4$ composite nanospheres are composed of two distinct components: the Fe_3O_4 shell composed of many fine primary magnetite nanocrystals was about 40 nm, and the black of Ag cores was about 45 nm. These nanostructures of $Ag@Fe_3O_4$ can overcome the aggregation of Ag nanoparticles, because the magnetic shell acts as a physical barrier to protect the Ag cores from irreversible aggregation [6]. As seen in Fig. 1b, e, it is obvious that the carbon-coated $Ag@Fe_3O_4$ composite nanospheres are perfectly spherical in shape with smooth surfaces and

Fig. 4 **a**–**e** The elemental mappings of C, O, Fe, Ag, and Au in the area shown in **f**. **g** EDX spectrum of $Ag@Fe_3O_4@C$-Au nanospheres

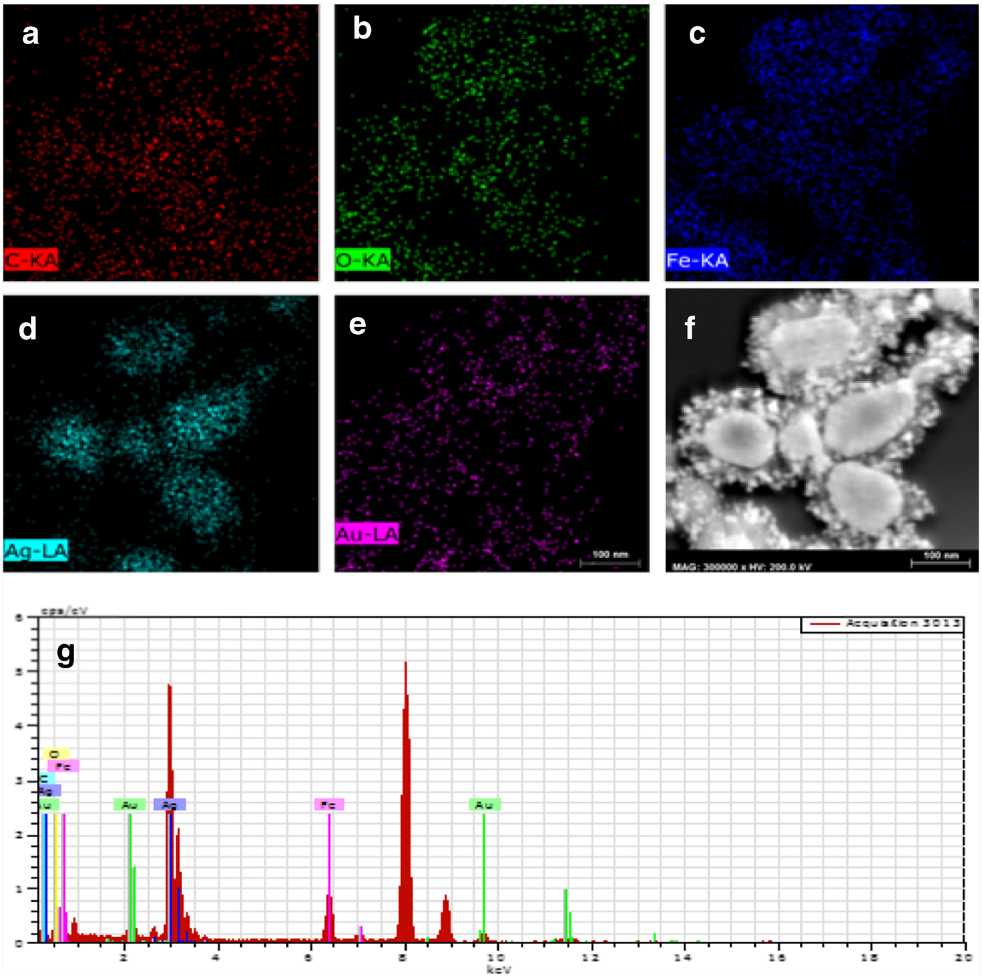

the shell layer of carbon is about 8 nm in thickness. The surface of the obtained Ag@Fe_3O_4@C composite microspheres was further modified by PEI to form sufficient amounts of amine functional groups, and the strong chemical bonding between Au atoms and N atoms in the amino groups ensures the grafting of Au NPs on the surface of Ag@ Fe_3O_4@C. After loading Au nanoparticles, the corresponding SEM and TEM images were shown in Fig. 1c, f; the whole Ag@Fe_3O_4@C-Au composite microspheres with the rough surface (a size of approximately 150 nm) are coated with about 16 nm Au nanoparticles. Thus, this triple core-shell-structured Ag@ Fe_3O_4@C-Au has a Fe_3O_4 magnetic embedded Ag core, an amorphous carbon coat, and a layer of Au nanoparticle shell.

The TGA curves of naked Ag@Fe_3O_4 and Ag@Fe_3O_4@C nanospheres were shown in Fig. 2. For naked Ag@Fe_3O_4, the TGA curve showed that the weight loss over the temperature range from 100 to 800°C was about 7.2%. This might be due to the loss of the removal of the remaining water and agents. Compared with the TGA curves of the naked Ag@Fe_3O_4, the Ag@Fe_3O_4@C nanospheres show that the main mass of the as-synthesized occurred about 40.0% decrease attributed to the decomposition of carbon coated on the surface of the Ag@Fe_3O_4 nanospheres.

The X-ray diffraction (XRD) patterns of the synthesized naked Fe_3O_4 nanospheres, Ag@Fe_3O_4, Ag@Fe_3O_4@C, and Ag@Fe_3O_4@ C-Au composite microspheres are shown in Fig. 3. For all the samples, six diffraction peaks at 30.08°, 35.42°, 43.08°, 53.56°, 57.0°, and 62.7° were indexed to the (220), (311), (400), (422), (511), and (440) planes of the Fe_3O_4 cubic inverse spinel phase. As shown in Fig. 3b for Ag@Fe_3O_4@C composite microspheres, four extra diffraction peaks at 38.2°, 44.3°, 64.4°, and 77.6° were indexed to the (111), (200), (220), and (311) planes of the Ag cubic phase (JCPDS no. 04-0783). As shown in Fig. 3c, d, these characteristic peaks can be seen in the composite magnetic nanoparticles, while the broad peak at 17–27° was ascribed to an amorphous carbon. According to the literature [6], the characteristic peaks for Au and Ag were too close to distinguish.

In order to further identify the formation of Ag@Fe_3O_4@C-Au microsphere composite, the samples were analyzed by electron mapping image analysis (Fig. 4). As can be seen in Fig. 4a–e, the Au, Ag, Fe, C, and O are distributed over the entire structure: Ag atoms are located in the core, Fe and O atoms are located in the shell of the Ag@Fe_3O_4 core-shell nanostructure, and C and Au nanoparticles are located in the outer surface of the Fe_3O_4 microspheres, respectively. Energy-dispersive X-ray spectroscopy (EDX) of an individual

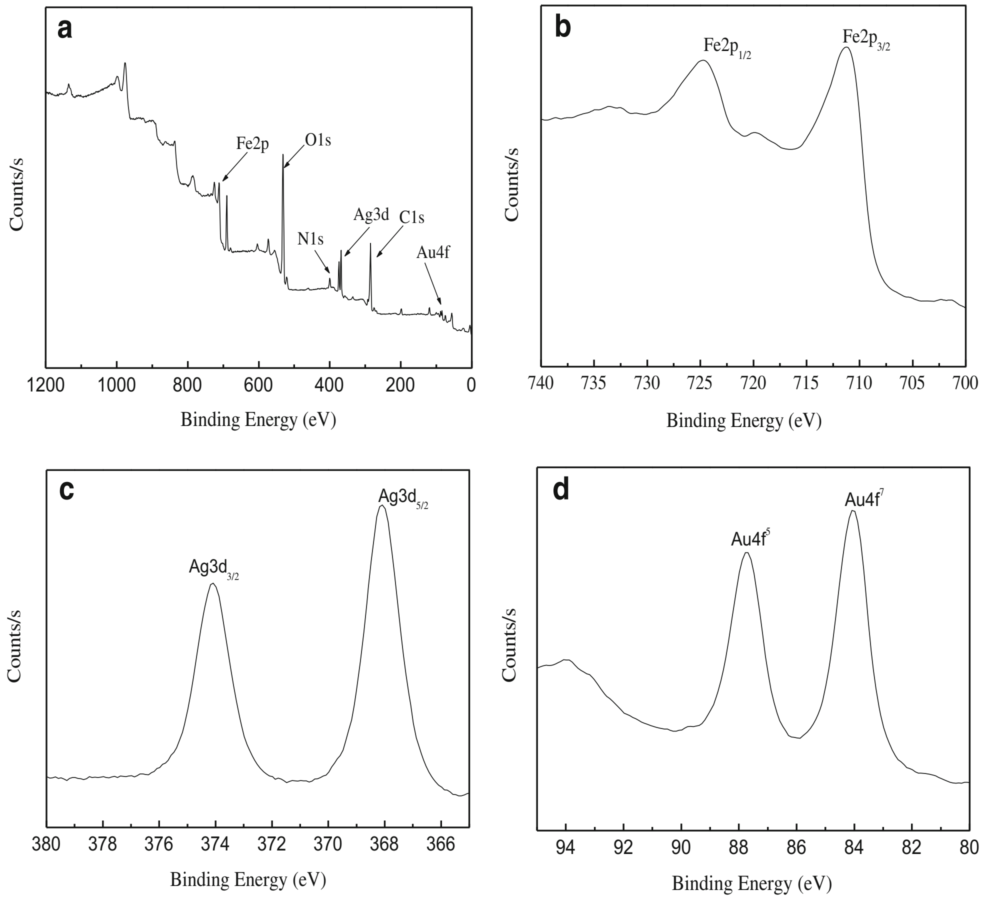

Fig. 5 XPS spectra of Ag@Fe_3O_4@C-Au composite microspheres: wide scan spectra (**a**), Fe 2p spectra (**b**), Ag 3d spectra (**c**), and Au 4f spectra (**d**)

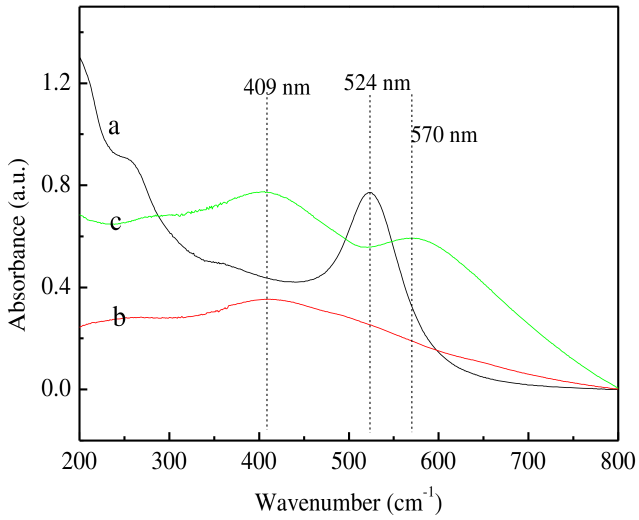

Fig. 6 UV-vis spectra of Au NPs (**a**), $Ag@Fe_3O_4$ (**b**), and $Ag@Fe_3O_4@C$-Au (**c**) microspheres

nanosphere in Fig. 4g shows that Ag, Au, Fe, C, and O peaks are presented in the spectra.

XPS analysis was performed on the $Ag@Fe_3O_4@C$-Au core-shell composite microspheres to gain a better understanding of the phase surface chemistry. Figure 5a shows the full scan spectra, which reveals the presence of silver, iron, oxygen, carbon, and nitrogen elements in the $Ag@Fe_3O_4@C$-Au composite microspheres. In the spectrum of Fe 2p (Fig. 5b), the peaks of Fe $2p_{1/2}$ and Fe $2p_{3/2}$ are located at 724.6 and 711.2 eV, respectively. In the Ag 3d spectrum (Fig. 5c), the binding energies of Ag $3d_{3/2}$ and Ag $3d_{5/2}$ with a peak splitting of 6 eV are 374.1 and 368.1 eV, respectively, which matches the standard reference XPS spectrum of metallic Ag. The $4f^5$ and $4f^7$ peaks of Au at 87.7 and 84.1 eV in Fig. 5d can be assigned to the metal Au.

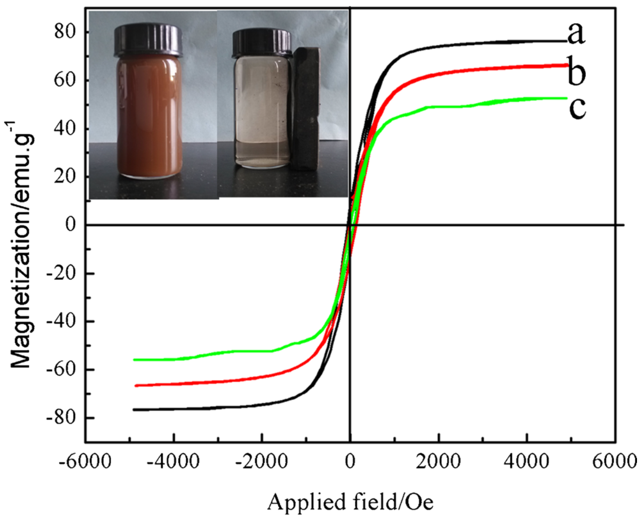

Fig. 7 Magnetization curves measured for $Ag@Fe_3O_4$ (**a**), $Ag@Fe_3O_4@C$ (**b**), and $Ag@Fe_3O_4@C$-Au (**c**) microspheres.

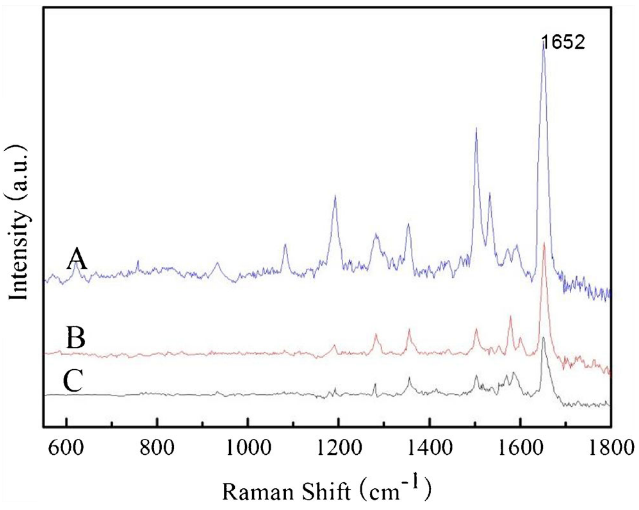

Fig. 8 SERS spectra of 10^{-6} M RdB on $Ag@Fe_3O_4@C$-Au microspheres (*A*), $Ag@Fe_3O_4$ microspheres (*B*), and $Fe_3O_4@C$-Au microspheres (*C*)

Figure 6 shows the UV-vis spectroscopy of Au, $Ag@Fe_3O_4$, and $Ag@Fe_3O_4@C$-Au composite microspheres. The $Ag@Fe_3O_4$ microspheres have an absorption peak at 409 nm because of the typical surface plasmon resonance of silver nanoparticles; the peak at 524 nm observed on Au nanoparticles was caused by the surface plasmon coupling between closely spaced Au nanoparticles. The absorption peak leads to a redshift to 570 nm after coating Au nanoparticles on the $Ag@Fe_3O_4@C$ microspheres. Thus, SERS measurements with 633-nm excitation have been extended to adsorbents on Au surfaces.

In addition, to gain a better understanding of the magnetic properties of the as-synthesized microspheres, the room-temperature magnetization saturation of the as-prepared $Ag@Fe_3O_4$, $Ag@Fe_3O_4@C$, and $Ag@Fe_3O_4@C$-Au particle

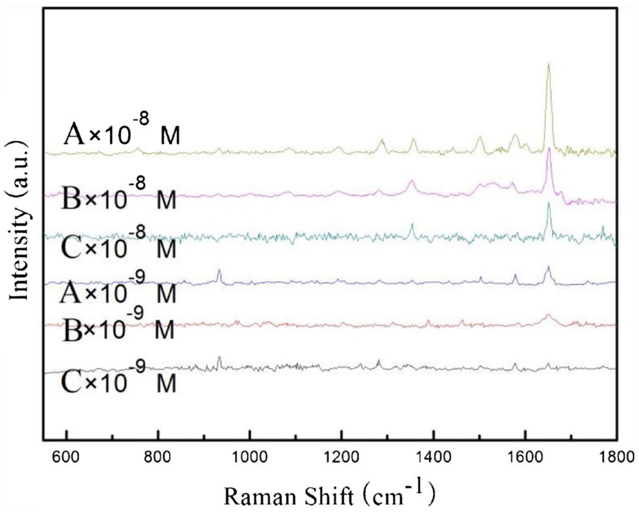

Fig. 9 SERS spectra of 10^{-8} M and 10^{-9} M RdB on $Ag@Fe_3O_4@C$-Au microspheres (*A*), $Ag@Fe_3O_4$ microspheres (*B*), and $Fe_3O_4@C$-Au microspheres (*C*)

values were measured in Fig. 7. The values of Ms of $Ag@Fe_3O_4$, $Ag@Fe_3O_4@C$, and $Ag@Fe_3O_4@$ C-Au particles were decreased to 76.3, 65.8, and 53.3 emu/g, successively. These phenomena can be explained by the diamagnetic contribution of the carbon shell and the Au nanoparticles surrounding $Ag@Fe_3O_4@C$ microspheres.

On the other hand, the $Ag@Fe_3O_4@C$-Au microspheres can be readily used as SERS substrates for molecular sensing with sensitivity and specificity. Because the core-shell microspheres have the Fe_3O_4 with magnetic properties and the novel metals were well-known SERS active materials, the $Ag@Fe_3O_4@C$-Au microspheres would be collected by magnet and also have SERS activity. In order to evaluate their performance as SERS substrates, we used RdB as the model SERS marker. Figure 8 presents the SERS spectra of 10^{-6} M RdB adsorbed on the surface of the $Ag@Fe_3O_4$, $Fe_3O_4@C$-Au, and $Ag@Fe_3O_4@C$-Au microspheres, respectively. As shown in Fig.8(A–C), the characteristic bands including $\nu_{CH(ip)}$ (1193 cm^{-1}) and $\nu_{C\text{-}C}$ (1356, 1503, 1580, and 1652 cm^{-1}) are observed, which is the Raman spectra of RB [6]. The $Ag@Fe_3O_4$ core-shell microspheres exhibit weak enhancement because of the electromagnetic damping of Fe_3O_4 shells on Ag (Fig. 8(B)), and the $Fe_3O_4@C$-Au microspheres possess weaker enhancement, which display that surface plasmon efficiency is greater for Ag than that for Au (Fig. 8(C)). The $Ag@Fe_3O_4@C$-Au microspheres cause a large increase in the intensity, which is larger than the other structure microspheres (Fig. 8(A)). In addition, compared with the $Fe_3O_4@C$-Au microspheres and $Ag@Fe_3O_4$ microspheres, the levels of SERS enhancement of these microspheres were measured. As shown in Fig. 9, it is clearly seen that the low concentrations of RdB (10^{-9}) in the solution can be detected by the $Ag@Fe_3O_4@C$-Au microspheres, but the other samples under the same concentration was almost undetectable. And the results are consistent with Fig. 8, which shows the SERS signals of RdB on the $Ag@Fe_3O_4@C$-Au microspheres were much stronger than those on both the $Ag@Fe_3O_4$ and $Fe_3O_4@C$-Au microspheres.

Conclusion

In conclusion, we have successfully synthesized novel multifunctional $Ag@Fe_3O_4@C$-Au magnetic core-shell microspheres that exhibit good sensitivity performance in SERS. The high SERS activities of the $Ag@Fe_3O_4@C$-Au composite microspheres have been utilized for the detection of low concentrations of RdB. Furthermore, due to their excellent magnetic properties, the microspheres can be reused with convenient magnetic separability.

Acknowledgments The authors gratefully acknowledge the support for this research from the Key Disciplines of Applied Chemistry of Zhejiang Province, Taizhou University, and the National Natural Science Foundation of China under Grant No. 21403150.

References

1. Fleischmann M, Hendra PJ, Mcquillan AJ (1974) Raman spectra of pyridine adsorbed at a silver electrode. Chem Phys Lett 26:163–166. doi:10.1016/0009-2614(74)85388-1
2. Fan M, Brolo AG (2009) Silver nanoparticles self assembly as SERS substrates with near single molecule detection limit. Phys Chem Chem Phys 34:7381–7390. doi:10.1039/b904744a
3. Zhang YY, Walkenfort B, Yoon JH, Schlucher S, Xie W (2015) Gold and silver nanoparticle monomers are non-SERS-active: a negative experimental study with silica-encapsulated Raman-reporter-coated metal colloids. Phys Chem Chem Phys 33:21120–21126. doi:10.1039/C4CP05073 H
4. Qi JW, Li D, Yang M, Wu Q, Chen ZQ, Wang WD, Lu WQ, Yu XY, Xu JJ, Sun Q (2013) Large-area high-performance SERS substrates with deep controllable sub-10-nm gap structure fabricated by depositing Au film on the cicada wing. Nanoscale Res Lett 8:437–482. doi:10.1186/1556-276X-8-437
5. Zhao Y, Zeng WC, Tao ZC, Xiong PH, Qu Y, Zhu YW (2015) Highly sensitive surface-enhanced Raman scattering based on multi-dimensional plasmonic coupling in Au-graphene-Ag hybrids. Chem Commun 51:866–869. doi:10.1039/c4cc07937j
6. Shen JH, Zhu YH, Yang XL, Zong J, Li CZ (2013) Multifunctional $Fe_3O_4@Ag/SiO_2/Au$ core-shell microspheres as a novel SERS-activity label via long-range plasmon coupling. Langmuir 29: 690–695. doi:10.1021/la304048v
7. Kim KH, Back YK, Jeon H, Srinivasarao M, Jung HT (2012) Cylindrical posts of $Ag/SiO_2/Au$ multi-segment layer patterns for highly efficient surface enhanced Raman scattering. Nanotechnology 31:1–5. doi:10.1088/0957-4484/23/31/315302
8. An Q, Zhang P, Li JM, Ma WF, Guo J, Hu J, Wang CC (2012) Silver-coated magnetite-carbon core-shell microspheres as substrate-enhanced SERS probes for detection of trace persistent organic pollutants. Nanoscale 4:5210–5216. doi:10.1039/c2nr31061a
9. Zhang XQ, Zhu YH, Yang XL, Zhou Y, Yao YF, Li CZ (2014) Multifunctional $Fe_3O_4@$ $TiO_2@Au$ magnetic microspheres as recyclable substrates for surface-enhanced Raman scattering. Nanoscale 6:5971–5979. doi:10.1039/c4nr00975d
10. Xu ZC, Hou YL, Sun SH (2007) Magnetic core/shell Fe_3O_4/Au and $Fe_3O_4/Au/Ag$ nanoparticles with tunable plasmonic properties. J Am Chem Soc 129:8698–8699. doi:10.1021/ja073057v
11. Zhang MF, Zhao AW, Wang DP, Sun HH (2015) Hierarchically assembled $NiCo@SiO_2@Ag$ magnetic core-shell microspheres as highly efficient and recyclable 3D SERS substrates. Analyst 140: 440–448. doi:10.1039/c4an01275e
12. Wang J, Song DQ, Zhang H, Zhang J, Zhang HQ, Zhou H, Sun Y (2013) Studies of $Fe_3O_4/Ag/Au$ composites for immunoassay based on surface plasmon resonance biosensor. Colloids Surf B: Biointerfaces 1:165–170. doi:10.1016/ j.colsurfb.2012.08.040
13. Jiang WQ, Zhou YF, Zhang YL, Xuan SH, Gong XL (2012) Superparamagnetic $Ag@Fe_3O_4$ core–shell nanospheres: fabrication, characterization and application as reusable nanocatalysts. Dalton Trans 41:4594–4601. doi:10.1039/c2dt12307j
14. Zhu MY, Diao GW (2011) Magnetically recyclable Pd nanoparticles immobilized on magnetic $Fe_3O_4@C$ nanocomposites: preparation, characterization, and their catalytic activity toward Suzuki and Heck coupling reactions. J Phys Chem C 115:24743–24749. doi:10.1021/jp206116e
15. Liu SH, Lu F, Liu Y, Jiang LP, Zhu JJ (2013) Synthesis, characterization, and electrochemical applications of multifunctional $Fe_3O_4@C$-Au nanocomposites. J Nanopart Res 15:1331–1339. doi:10.1007/ s11051-012-1331-5